



TITLE:

Relationship between surface velocity divergence and turbulence microscale in open-channel flows with submerged strip roughness

AUTHOR(S):

Okamoto, T; Sanjou, M; Nezu, I

CITATION:

Okamoto, T ...[et al]. Relationship between surface velocity divergence and turbulence microscale in open-channel flows with submerged strip roughness. IOP Conference Series: Earth and Environmental Science 2016, 35(1): 012015.

ISSUE DATE:

2016-05-20

URL:

<http://hdl.handle.net/2433/252303>

RIGHT:

Content from this work may be used under the terms of the Creative Commons Attribution 3.0 licence. Any further distribution of this work must maintain attribution to the author(s) and the title of the work, journal citation and DOI.

PAPER • OPEN ACCESS

Relationship between surface velocity divergence and turbulence microscale in open-channel flows with submerged strip roughness

To cite this article: T Okamoto *et al* 2016 *IOP Conf. Ser.: Earth Environ. Sci.* **35** 012015

View the [article online](#) for updates and enhancements.

Related content

- [Relationship between surface velocity divergence and gas transfer in open-channel flows with submerged simulated vegetation](#)
M Sanjou, T Okamoto and I Nezu
- [Dispersion in open-channel flow subject to the processes of sorptive exchange on the bottom and air–water exchange on the free surface](#)
Chiu-On Ng
- [Instability of shallow open channel flow with lateral velocity gradients](#)
A C Lima and N Izumi

Relationship between surface velocity divergence and turbulence microscale in open-channel flows with submerged strip roughness

T Okamoto, M Sanjou and I Nezu

Department of Civil and Earth Resources Engineering, Kyoto University, Kyoto, Japan

E-mail: takaaki.okamoto@water.kuciv.kyoto-u.ac.jp

Abstract. The present study investigates the effects of strip roughness on surface velocity divergence (SD) to develop physical modelling of gas transfer mechanisms in natural rivers. Particularly, turbulence measurements were conducted by PIV in a computer-controlled laboratory flume with varying water discharge and roughness spacing systematically, in order to obtain the space and time distributions of surface velocity divergence, turbulent kinetic energy and dissipation rate on the horizontal plane. Finally, a new empirical model for the surface velocity divergence was proposed considering turbulence microscales.

1. Introduction

McCready *et al.* [3] report that the surface velocity divergence (SD) is relevant to gas transfer processes at the air-water boundary. Therefore, the SD is highlighted in the gas transfer studies. The present study focuses on two-dimensional rough-bed flows, in which strip roughness elements are placed with constant spacing. It is well known that shedding vortices produced periodically behind the roughness element are transported toward the free surface. Although previous studies (Djenidi *et al.* [2], Pokarajac *et al.* [6]) point out that turbulence structure depends significantly on a ratio of roughness spacing to roughness height, many uncertainties remain about the relation between the SD and the coherent turbulence induced by the rough bed.

In this study we investigated hydrodynamic effects of strip roughness on the SD to develop physical modelling of gas transfer mechanisms in natural rivers. Particularly, turbulence measurements were conducted by PIV in a computer-controlled laboratory flume with varying water discharge, flow depth and roughness spacing systematically, in order to obtain the space and time distributions of SD, turbulent kinetic energy and dissipation rate. Finally, a new empirical model for the SD in natural rivers was proposed considering turbulence structure.



Table 1. Hydraulic conditions

	ϕ	U_m (cm/s)	U_s (cm/s)	k_L (cm/s)	T_w (°C)	H (cm)	H/h
Case1-1	0.0	5.0	7.0	0.0013	24.6	12.0	8.0
Case1-2		10.0	13.3	0.0023	23.6		
Case1-3		20.0	24.3	0.0048	24.0		
Case2-1	3.0	5.0	7.4	0.0014	19.7		
Case2-2		10.0	14.8	0.0025	18.7		
Case2-3		20.0	27.4	0.0065	19.6		
Case3-1	5.0	5.0	7.1	0.0023	20.4		
Case3-2		10.0	13.2	0.0036	19.1		
Case3-3		20.0	27.4	0.0069	20.1		
Case4-1	8.0	5.0	6.0	0.0025	19.9		
Case4-2		10.0	14.2	0.0046	20.1		
Case4-3		20.0	32.6	0.0073	20.3		
Case5-1	12.0	5.0	7.2	0.0024	20.6		
Case5-2		10.0	14.9	0.0047	19.7		
Case5-3		20.0	30.2	0.0081	19.8		
Case6-1	16.0	5.0	7.3	0.0019	19.5		
Case6-2		10.0	13.8	0.0032	18.7		
Case6-3		20.0	30.8	0.0067	18.6		

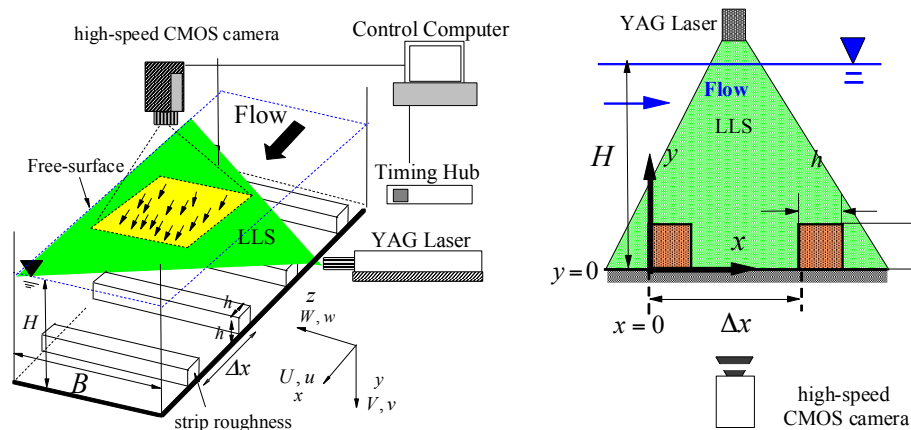


Figure 1. (left) Horizontal PIV system and (right) vertical PIV system

2. Measurement methods

Figure 1 shows the experimental set-up and the coordinate system. The experiments were conducted in a 16-m long and 40-cm wide glass flume. Streamwise, vertical and spanwise coordinates are x , y and z , respectively. The vertical origin, $y = 0$ was chosen as the channel bed. The time-averaged velocity components in each direction are defined as U , V and W , and the corresponding turbulent fluctuations are u , v and w , respectively. The strip roughness elements were placed on the flume bed with constant spacing in the streamwise direction. The roughness elements used were two-dimensional regular transverse square bars. The roughness height was $h = 15.0$ mm.

The measured region was located at about 7 m downstream from the channel entrance and the turbulent flow was fully developed. The 2.0-mm thick LLS (laser light sheet) was generated by a 3.0-W YAG laser using a cylindrical lens. The LLS was projected horizontally and vertically with a spatial resolution of about 0.29 mm per pixel. The LLS plane was illuminated together with tracer particles (diameter of 0.1 mm and specific density of 1.02) and captured by a high-speed CMOS camera. The instantaneous velocity vectors (\tilde{u} , \tilde{w}) were calculated by a PIV algorithm [5]. The PIV analysis was conducted by direct correlation, in which the interrogation window size was 25×25 pixels. When the correlation value between the first and second image patterns was less than 0.4, a local velocity vector was judged as an invalid vector, and interpolated velocity data were given to the corresponding position using surrounding valid vectors.

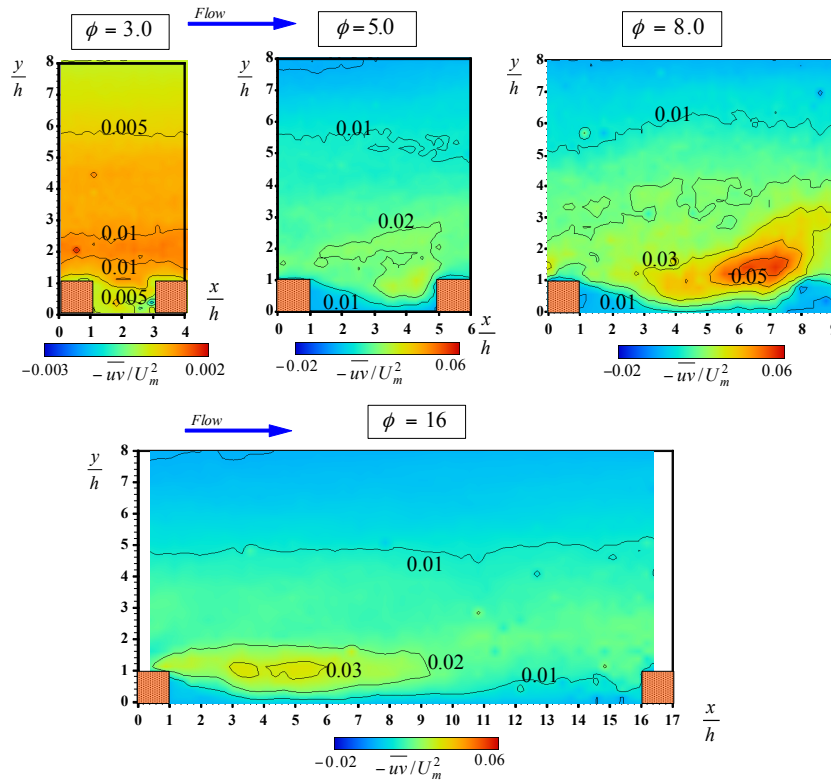


Figure 2. Contours of Reynolds stress by vertical PIV ($U_m = 10$ cm/s).

Table 1 shows the hydraulic conditions, in which U_m is the bulk mean velocity and U_s is the surface streamwise velocity in the centerline of the flume. $\phi \equiv \Delta x/h$ is a relative spacing of strip roughness elements, in which Δx is a streamwise distance between the neighboring roughness elements. The LLS positions are $y/H = 0.98$ for the horizontal PIV. The gas transfer velocity K_L was measured using two dissolved oxygen meters [4].

3. Results and discussion

3.1. Turbulence structure and surface divergence distribution for rough bed flow

Figure 2 shows the contours of the Reynolds stress $-\overline{uv}$ for $\phi = 3.0, 5.0, 8.0$ and 16.0 . The values of $-\overline{uv}$ are normalized by the square of the bulk mean velocity U_m^2 . Note that the Reynolds stress contours have the peak value at the canopy edge ($y/h = 1.0$). As the coherent structure develops between elements, the peak values of $-\overline{uv}_{peak}(x)$ become larger downstream. It is also observed that for $\phi = 3.0-8.0$, the magnitude of the Reynolds stresses in the outer layer increases in proportion to the roughness spacing ϕ . In contrast, for $\phi = 16.0$, the Reynolds stress peak is located at $x/h = 6.0$. It is also observed that the Reynolds stress values become smaller as the flow approaches the next roughness element.

Figure 3 shows the contours of instantaneous surface velocity divergence $\tilde{\beta}$ and velocity vectors (\tilde{u}, \tilde{w}) on the horizontal plane ($y/H = 0.98$) in the cases of $U_m = 10$ cm/s for $\phi = 5.0$. The longitudinal positions of the roughness are indicated in figure 2. The velocity vectors are drawn in a movable coordinate subtracting the bulk-mean velocity U_m . $\tilde{\beta} < 0$ yields a convergence zone where momentum concentrates and is accompanied by a downward current. In contrast, $\tilde{\beta} > 0$ yields a divergence zone where upward current transferred from the flume bed results in momentum divergence.

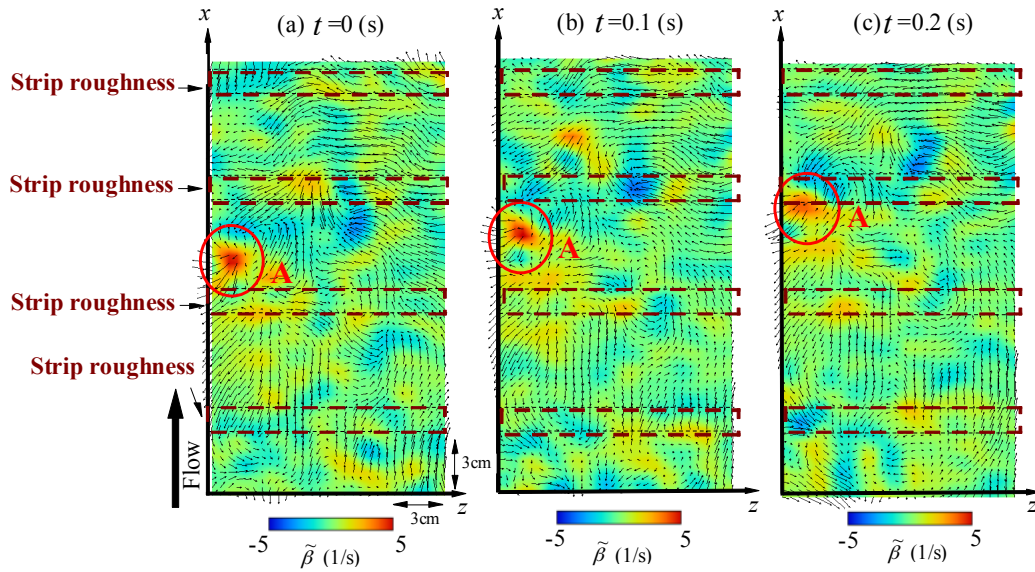


Figure 3. Time-series of the surface velocity divergence on the horizontal plane near the free surface ($U_m = 10$ cm/s, $\phi = 5$).

$$\tilde{\beta} \equiv \frac{\partial \tilde{u}}{\partial x} + \frac{\partial \tilde{w}}{\partial z} = -\frac{\partial \tilde{v}}{\partial y} \quad (1)$$

From the contour of instantaneous surface divergence, the positive and negative divergence zones appear periodically (figure 3). In blue and red circles accompanied by large divergence values, we can distinguish the divergence and convergence zones of the free surface fluid by the direction of velocity vectors. The circle 'A' is transferred downstream, keeping its formation. Note that the convection velocity does not depend on the strip roughness position.

3.2. Effects of roughness spacing on surface divergence

Figure 4 shows the relationship between the gas transfer velocity k_L and the divergence intensity. McCready *et al.* [3] propose a surface divergence (SD) model as follows:

$$k_L = \alpha \sqrt{D \beta'} \quad (2)$$

in which D is molecular diffusivity of dissolved oxygen in water and $\beta' = \sqrt{(\tilde{\beta} - \bar{\beta})^2}$ ($\bar{\beta}$: time-averaged surface velocity divergence) is the RMS value of the instantaneous SD, and α is a proportional coefficient. The linear relation is observed for flows with strip roughness and α ranges from 0.3 to 0.5.

Figure 5 shows the relationship between the roughness spacing and the divergence intensity. Note that a single peak appears at $\phi = 12$, irrespective of the bulk-mean velocity U_m . Coleman *et al.* [1] report that the vortex strength formed over the roughness strip becomes larger when the relative spacing is

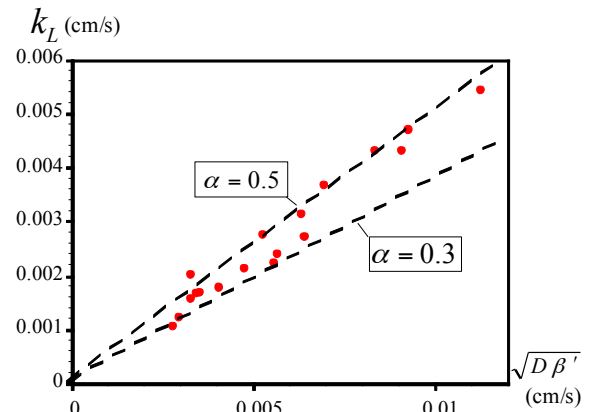


Figure 4. Relation between gas transfer velocity and the surface divergence intensity.

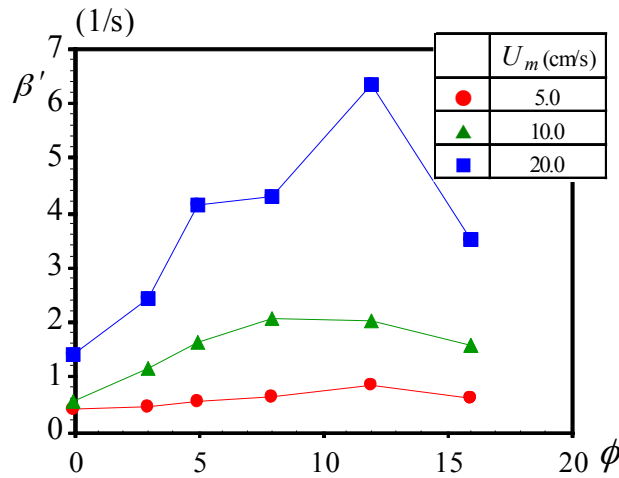


Figure 5. Relation between intensity of surface velocity divergence and relative spacing of strip roughness.

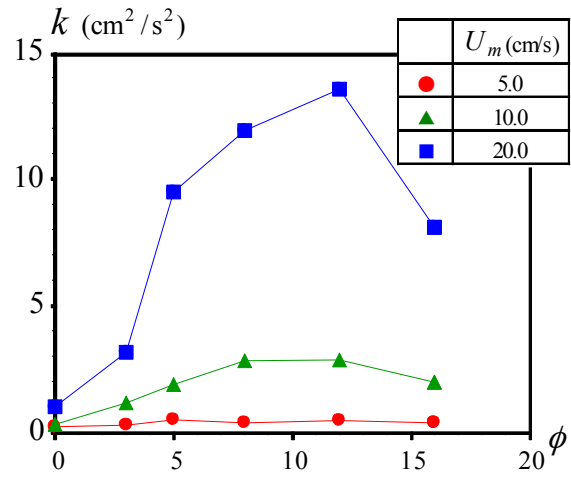


Figure 6. Relation between turbulent kinetic energy and relative spacing of strip roughness.

about $\phi = 8$ (see figure 2). It is thus inferred that the SD has a strong relation with the turbulent structures induced by rough-bed flow. Furthermore, the results revealed that the values of the SD become larger in high velocity conditions. This suggests that the Reynolds number may be a key factor on the production of the surface divergence.

It is generally difficult to measure the SD because we have to obtain the time-series of the velocity components (\tilde{u}, \tilde{w}) on the horizontal plane simultaneously. But the turbulence statistics, such as the turbulent kinetic energy and dissipation rate, can be analyzed using a single-point measurement method. Therefore, correlating the turbulence statistics and the surface divergence will contribute to the development of practical and useful prediction methods for the surface divergence and the related gas transfer velocity.

3.3. Turbulent kinetic energy

Figure 6 shows the relationship between the roughness spacing and the turbulent kinetic energy k . Turbulent kinetic energy k is defined as follows:

$$k = \frac{1}{2} (u'^2 + w'^2) \quad (3)$$

u' is the RMS value of the instantaneous streamwise velocity \tilde{u} , and w' is the RMS value of the instantaneous spanwise velocity \tilde{w} . The turbulent kinetic energy has a single peak at $\phi = 12$. This is in good agreement with figure 5 (the surface velocity divergence). Coleman *et al.* [1] conducted turbulence measurements and report that the Reynolds stress value reaches a maximum for $\phi = 8$. Our results are in good agreement. In cases of large relative spacing ($\phi = 16$), local turbulence structures are produced behind the roughness element, but they become smaller and disappear with distance from the roughness element (figure 2). In the cases of small roughness spacing, the spacing is smaller than the flow separation length and the turbulence structure does not develop between the roughness elements. Consequently, the mean flow and turbulence structures become uniform in the streamwise direction and near the wall boundary condition.

3.4. Physical modeling of SD with Kolmogorov scale

The turbulent dissipation rate ε is the transfer rate from turbulence energy toward heat per unit mass and time, which is often calculated by using Kolmogorov's scale.

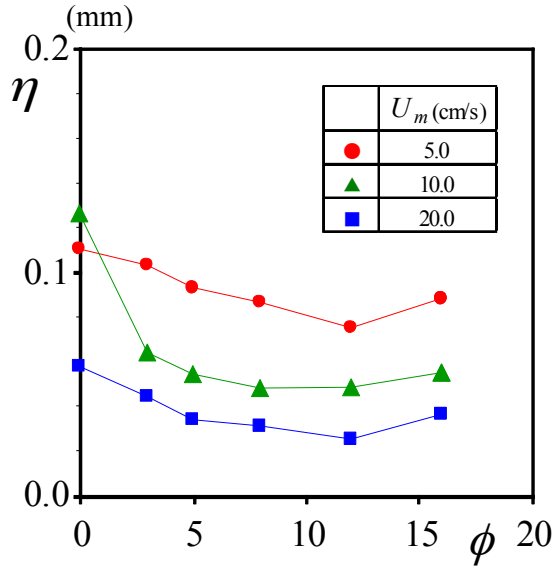


Figure 7. Relation between Kolmogorov length scale and relative spacing of strip roughness.

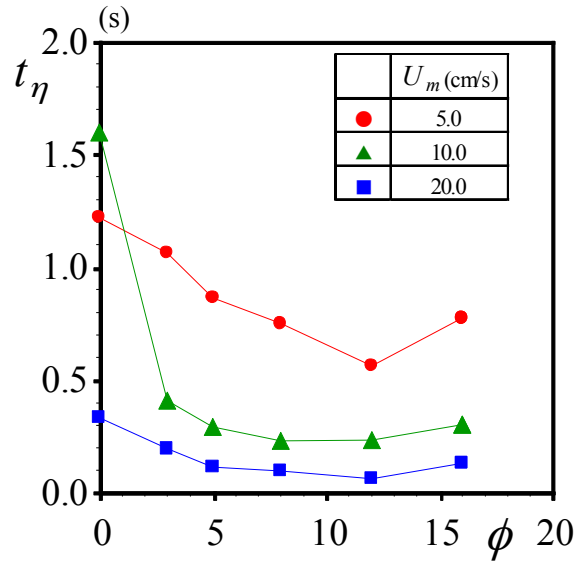


Figure 8. Relation between Kolmogorov time scale and relative spacing of strip roughness.

$$\frac{\varepsilon}{\nu} \equiv \frac{1}{2} \overline{\left(\frac{\partial u_i}{\partial x_j} + \frac{\partial u_j}{\partial x_i} \right)^2} \quad (4)$$

The present study evaluates it from the original definition because time series of velocity components could be obtained simultaneously for the multi-measured points. Here, we consider the dissipation rate on the free surface. The continuity equation leads to the following.

$$\frac{\partial v}{\partial y} = - \left(\frac{\partial u}{\partial x} + \frac{\partial w}{\partial z} \right) \quad (5)$$

Under the low Froude number condition, $v = 0$ and $\partial u / \partial y = \partial w / \partial y = 0$ can be assumed on the free surface. Combining equations (4) and (5) yields the following.

$$\frac{\varepsilon}{\nu} = 4 \overline{\left(\frac{\partial u}{\partial x} \right)^2} + 4 \overline{\left(\frac{\partial w}{\partial z} \right)^2} + 4 \overline{\left(\frac{\partial u}{\partial x} \right) \left(\frac{\partial w}{\partial z} \right)} + \overline{\left(\frac{\partial u}{\partial z} + \frac{\partial w}{\partial x} \right)^2} \quad (6)$$

The right-hand side terms are calculated using measured two-dimensional PIV data.

Under Kolmogorov's local isotropy hypothesis, a probability density function of turbulence is defined by the viscous coefficient ν and turbulent energy dissipation ε . The characteristic length is obtained by these physical variables as indicated by equation (7). This corresponds to the length scale of minimal turbulent vortex. In the same way, a characteristic time scale could be defined by equation (8).

$$\eta \equiv \left(\frac{\nu^3}{\varepsilon} \right)^{1/4} \quad (7)$$

$$t_{\eta} = \left(\frac{\nu}{\varepsilon} \right)^{1/2} \quad (8)$$

Figure 7 compares the Kolmogorov length among the different hydraulic conditions. The Kolmogorov length scale is smaller for a rough bed than for a smooth bed flow ($\phi = 0$). It reaches a minimum at $\phi = 12$ and increases slightly between $\phi = 12$ and 16. Figure 8 shows the relation between the roughness spacing and the Kolmogorov time scale. The same trend is observed as for the length scale (figure 7). These results suggest that both length and time scales become larger when turbulence production is comparatively small, and in contrast, they become smaller when greater turbulence is formed.

Figure 9 shows the relation between the time scale and the SD. A distinct linear relation is observed, as given by equation (9).

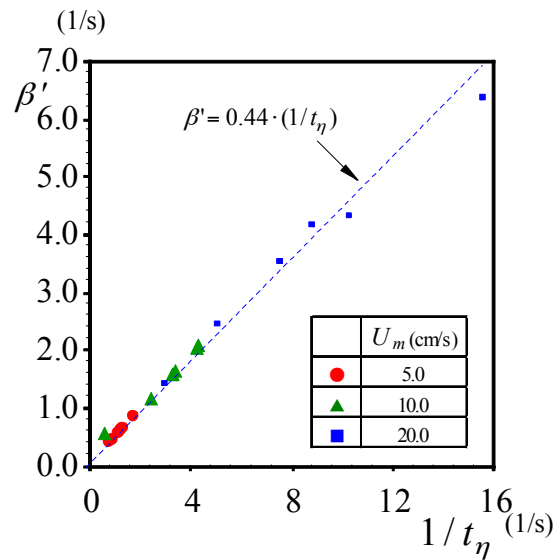


Figure 9. Linear relation between the Kolmogorov time scale and the surface divergence intensity.

$$\beta' = 0.44 \cdot (1/t_{\eta}) \quad (9)$$

The scatter of the measured data is small, making it more useful for the physical modelling.

4. Conclusions

We focused on the surface velocity divergence (SD) in open-channel flows with strip roughness. The horizontal PIV measurements obtained a time series of free-surface velocity divergence. Positive and negative divergence zones are transferred downstream with time in the same manner as the boil phenomena in a natural river surface.

The SD intensity relates with turbulence statistics, irrespective of the streamwise spacing of roughness elements. A distinct linear relation between the SD intensity and turbulence microscales, such as Kormogorov's scale, was observed for rough-bed flow.

References

- [1] Coleman S *et al* 2007 *J. Engineering Mechanics* **133** 194
- [2] Djenidi L *et al* 2008 *Exp. Fluid* **44** 37
- [3] McCready M J *et al* 1986 *AIChE J.* **32** 1108
- [4] Moog D B and Jirka G H 1999 *J. Hydraulic Eng.* **125** 3
- [5] Nezu I and Sanjou M 2011 *J. Hydro-environment Res.* **5** 215
- [6] Pokarajac D *et al* 2008 *Exp. Fluids* **45** 73